Catalysis with Competitive Reactions: Static and Dynamical Critical Behavior

E. C. da Costa

Núcleo de Pesquisa em Eliminação de Resíduos de Processos Produtivos, UNISUL

Campus da Grande Florianópolis, Unidade II, 88130-000, SC, Brazil

and W. Figueiredo

Departamento de Física, Universidade Federal de Santa Catarina

88040-900, Florianópolis, SC, Brazil

Received on 11 April, 2003

We studied in this work a competitive reaction model between monomers on a catalyst. The catalyst is represented by hypercubic lattices in $d = 1$, 2 and 3 dimensions. The model is described by the following reactions: $A + A \rightarrow A_2$ and $A + B \rightarrow AB$, where A and B are two monomers that arrive at the surface with probabilities y_A and y_B, respectively. The model is studied in the adsorption controlled limit where the reaction rate is infinitely larger than the adsorption rate. We employ site and pair mean-field approximations as well as static and dynamical Monte Carlo simulations. We show that, for all d, the model exhibits a continuous phase transition between an active steady state and a B-absorbing state, when the parameter y_A is varied through a critical value. Monte Carlo simulations and finite-size scaling analysis near the critical point are used to determine the static critical exponents β, $\nu_\perp$ and the dynamical critical exponents $\nu_{||}$, δ, η and z. The results found for this competitive reaction model are in accordance with the conjecture of Grassberger, which states that any system undergoing a continuous phase transition from an active steady state to a single absorbing state, exhibits the same critical behavior of the directed percolation universality class.

I Introduction

In the course of the last decade the statistical mechanics community has made great progress in the study of nonequilibrium phenomena. Until now, we do not have a complete theory accounting for the nonequilibrium systems. The fundamental concept of a Gibbsian distribution of states in equilibrium has no counterpart in the nonequilibrium situation. This happens because many of these systems do not present even an hamiltonian function and, if it is possible to define an hamiltonian, the detailed balance would be violated.

Examples of recent problems on nonequilibrium processes include markets [1, 2], rain precipitation [3], sandpiles [4] and conserved contact process [5]. There is also a great interest in modeling interface growth [6, 7], traffic flow [8], temperature dependent catalytic reactions [9], etc. Nonequilibrium magnetic systems, with a well defined hamiltonian, have been also studied in the context of nonequilibrium processes [10, 11] as well.

For the equilibrium systems we can induce phase transitions by changing some external parameters. Usually, the temperature is the selected control parameter to study phase transitions between equilibrium states. In the case of continuous phase transitions, at the critical point, long range correlations are established inside the system and a set of critical exponents can be defined to describe the critical behavior of some thermodynamic properties. The renormalization group theory [12] is a well known theory that allows the calculation of these critical exponents.

We can also consider external constraints for the nonequilibrium systems that can drive the dynamical behavior of the system. The nature of the external parameter depends on the nature of the system. For instance, in an epidemic model for the spread of a disease, the external parameter to be considered is the rate of change of the healthly individuals into unhealthly ones. In a catalytic reaction model, the external parameter can be the rate of change of the concentration of reactants. These, and many other examples of nonequilibrium systems display dynamical phase transitions. A comprehensive survey on the dynamic phase transitions can be found in the books of Marro and Dickman [13] and Privman [14].

Catalytic reaction models are a class of nonequilibrium systems that show phase transitions among its stationary states. Particularly, these are irreversible phase transitions (IPR). Since the pioneering work of Schlögl [15] and Ziff, Gulari and Barshad [16], many other catalytic reaction models appeared in literature [17].

Recently, we have proposed a reaction model between monomers on a catalytic surface [18, 19] that can be viewed as a mixture of two other models: the $A + A \rightarrow A_2$ autocatalytic reaction model and the $A + B \rightarrow AB$ monomer-monomer reaction model.

The monomer-monomer reaction model [20, 21] is the simplest catalytic reaction model, described by the reaction $A + B \rightarrow AB$, where A and B are two monomers that arrive on a surface with probabilities y_A and $y_B = 1 - y_A$, respectively. This model was studied in the reaction controlled limit as well as in the adsorption controlled limit. In both cases, if $y_A > 0.5$, the surface becomes saturated by monomers A, and the system always enters into an absorbing state. On the other hand, if $y_A < 0.5$, the absorbing state is one in which the lattice is completely covered by monomers of the type B. However, if $y_A = 0.5$, the surface still saturates but with a much slower rate, and there is no preferred species to saturate the catalyst. The mapping onto the kinetic Ising model [22] showed that the time for the system to enter the absorbing state, at the particular value $y_A = 0.5$ and, in the reaction controlled limit, grows with the system size. Studies including monomers with different sizes [23], substrate viewed as a complete graph [24], introduction of a repulsive interaction between like monomers [25], the increase in the number of degrees of freedom for the reaction [26], are some examples of the research concerning the monomer-monomer reaction model carried out in the last decade.

On the other hand, the autocatalytic model [27] can be described by the reaction $A+A \rightarrow A_2$. This model was also considered by Aukrust, Browne and Webman [28], where they introduced a probability reaction between two adsorbed A monomers that occupy nearest neighbor sites on the lattice. Their model presents a continuous phase transition from a reactive steady state into an absorbing state, and the critical behavior of the model is in the same universality class of the Directed Percolation. Through Monte Carlo simulations and finite size scaling analysis, they were able to find the static critical exponents of the model.

In our model, the catalyst was represented by a hypercubic lattice, and it is in contact with an infinite reservoir of monomers A and B in their gaseous phases. The monomers A and B arrive at the surface with probabilities y_A and $y_B = 1-y_A$, respectively. These probabilities are related to the partial pressures of the gases A and B inside the reservoir. The model was investigated by effective field approximations, as well as through static and dynamic Monte Carlo simulations in $d = 1$, 2 and 3 dimensions. The static critical behavior exhibited by the model in two dimensions [18] put it in the same universality class of the Directed Percolation (DP). This was indeed expected, because the model presents a single continuous transition from a reactive stationary state into an absorbing state, and the rate equations that describe the evolution of the system can be mapped onto those of the contact process. The dynamical critical behavior of the model in two dimensions [19] was also investigated and we calculated the dynamical critical exponents δ, η and z, which control the asymptotic behavior of the survival probability, the number of empty sites (the order parameter of the model) and the mean square displacement of vacancies from the origin, respectively. For the calculation of the dynamical critical exponents, the simulations started with the lattice covered by monomers of the type B, except in a central site, that is left empty. Thus, the configuration of the system in the beginning of the simulations is very close to the absorbing state. That study was made by employing an epidemic analysis [29-31]. The dynamical critical exponents of the model are the same as those of Directed Percolation.

The DP universality class is the paradigm to describe the nonequilibrium phase transitions of a variety of models. However, the experimental determination of the critical exponents is too hard. In real systems, a perfect absorbing state is not easily realized because there are always small fluctuations, for instance, due to thermal desorption of the elements. The presence of impurities, inactive sites and other inhomogeneities on the catalyst also difficult the measurements of the critical exponents. A full account on the possible experimental realizations of Direct Percolation can be found in the review work of Hinrichsen [32] and the references therein.

In the present work our main task is to extend the results found in two dimensions for the competitive reaction model to one and three dimensions. We present results obtained by employing mean field approximations, as well as static and dynamic Monte Carlo simulations. The model also exhibits continuous phase transition into an absorbing state, and the finite-size scaling arguments show that the model belongs to the same universality class of the Directed Percolation in all the dimensions considered in this work. This paper is organized as follows: in the next section we describe the model and we present the results obtained through the site and pair mean-field approximations in one, two, and three dimensions. In section III the model is studied by using static Monte Carlo simulations and finite-size scaling arguments. Section IV is dedicated to the study of the dynamical critical behavior of the model. In the last section we present our main conclusions.

II Model and mean-field approximations

We consider a catalytic surface in contact with an infinite reservoir of monomers, labeled by A and B. The catalyst will be represented by a linear chain, as well as by square and cubic lattices. These monomers can be adsorbed onto the lattice, and they can react according to the following steps:

(i) $A_{(g)} + v \rightarrow A_{(a)}$,

(ii) $B_{(g)} + v \rightarrow B_{(a)}$,

(iii) $A_{(a)} + A_{(a)} \rightarrow A_{2_{(g)}}$,

(iv) $A_{(a)} + B_{(a)} \rightarrow AB_{(g)}$.

The first two steps describe the adsorption of the species, and the other two, the possible reactions between adsorbed monomers that occupy nearest neighbor sites. Here, the (g) and the (a) labels denote a monomer in the gaseous and in the adsorbed phases, respectively. The symbol v indicates a vacant site. The rules $(i) - (iv)$ can also describe a lattice model for the birth and death of vacancies, resembling to the contact process. For instance, the processes (i) and (ii) account for the annihilation of a vacancy due to the adsorption of a particle, while the processes (iii) and (iv) give the birth of a vacancy due to the reaction step. For these reactions to occur, we need to have at least one vacant site, which is nearest neighbor of an adsorbed monomer. After the reaction, a pair of nearest-neighbor vacant sites is generated on the surface. In this way, we could resume the four steps above by a simple birth-death process for vacancies: $v \rightarrow \emptyset$ and $v \rightarrow 2v$. Then, we expect that our model is in the same universality class of the contact process [13], which belongs to the universality class of the DP.

It is convenient to introduce the following variables to describe the probabilities of the reactions:

$$\Pi_{AA} = \frac{N_A}{N_A + N_B} \quad ; \quad \Pi_{AB} = \frac{N_B}{N_A + N_B} \ . \qquad (1)$$

If a monomer of the type A adsorbs on an empty site surrounded by N_A monomers of the type A and N_B monomers of the type B, it will react with anyone of the A monomers with the probability Π_{AA}. In other words, Π_{AA} gives the probability of the occurrence of the $A + A$ reaction in the presence of B monomers [33]. We must also introduce the quantity y_A, which gives the probability that the next arriving monomer to be of the A species. For the B monomers the probability is y_B. These parameters are related to the ratio of the partial pressures of the gases A and B inside the reservoir. Due to the fact that the partial pressures are normalized, we have $y_A + y_B = 1$. Thus, the model has only a single independent parameter, y_A. The dynamics of the model can be thought as **a)** the transport of monomers to the substrate, **b)** adsorption of the monomers onto the catalytic surface, **c)** surface reaction between adsorbed monomers, **d)** desorption of the products (the dimers) and **e)** transport of the products away the catalytic surface. Because we assumed an infinite reservoir of monomers, the steps **a)** and **e)** occur instantaneously. In our modeling, we also consider that the steps **b)** and **d)** are irreversible, and it is also supposed that the adsorbed monomers cannot diffuse on the lattice. We studied the model in the adsorption controlled limit, where the rate for the reactions is much larger than the rate for the adsorption.

A. Site approximation

In the site mean field approximation we neglect the correlations between neighboring sites, and we take all of them as being statistically independent. We consider that the system is translationally invariant. In this way, we define the densities $p_i = N_i/N$ as being the number of sites occupied by the species i divided by the total number N of sites in the lattice. The label i stands for the A and B monomers, as well as for the vacant (v) sites in the lattice. The densities are normalized,

$$p_A + p_B + p_v = 1 \ . \qquad (2)$$

Now, we need to calculate the transition probabilities describing the steps (i) to (iv) presented before. In the table I we show the balance of the vacant sites.

Table I. Steps describing the processes (i) to (iv) in the site mean field approximation.

1. $A + v \rightarrow A_{ads.}$	2. $A + v \rightarrow A_2 \uparrow +2v$	3. $A + v \rightarrow AB \uparrow +2v$
4. $B + v \rightarrow B_{ads.}$	5. $B + v \rightarrow AB \uparrow +2v$	

For instance, for the process 1, an A monomer in the gaseous phase arrives at an empty site and sticks there if all its neighboring sites are empty. On the other hand, for the process 2, an A monomer in the gaseous phase arrives at an empty site and finds at least one A monomer adsorbed in its neighborhood. Then, they react instantaneously, forming the dimer A_2, that immediately leaves the catalyst, and two new vacant sites are left on the surface. The time evolution of the densities is described by a set of differential equations that takes into account the five processes considered in the table I:

1. The rate for this process can be given by

$$T_1 = y_A p_v^{\alpha+1} \ , \qquad (3)$$

where α is the coordination number of the lattice.

2. To calculate the rate for this process we must consider all the possible configurations around the empty site where the A monomer arrives. The table II lists all the combinations of A and B monomers.

The rate for this process can be written in the following form

$$T_2 = y_A p_v \sum_{j=1}^{\alpha} \sum_{i=0}^{\alpha-j} C_{\alpha,j}\, C_{\alpha-j,i}\, p_A^j\, p_B^i\, p_v^{\alpha-i-j} \left(\frac{j}{i+j}\right) \ , \tag{4}$$

where $C_{\alpha,j}$ stands for the combinatorics.

3. Analogously to the previous case, the rate for this process is

$$T_3 = y_A p_v \sum_{j=1}^{\alpha} \sum_{i=0}^{\alpha-j} C_{\alpha,j}\, C_{\alpha-j,i}\, p_A^i\, p_B^j\, p_v^{\alpha-i-j} \left(\frac{j}{i+j}\right) \ . \tag{5}$$

4. In this case the rate is

$$T_4 = y_B p_v \left(p_v + p_B\right)^{\alpha} \ . \tag{6}$$

Table II. Possible distributions of A and B monomers around an empty site where there is an A monomer arriving. The configurations listed in each column give the number of A monomers and the possible distributions of B monomers in a lattice of coordination number α.

$1\,A$ $\left\{\begin{array}{c} 0\,B \\ 1\,B \\ 2\,B \\ \vdots \\ (\alpha-1)\,B \end{array}\right\}$	$2\,A$ $\left\{\begin{array}{c} 0\,B \\ 1\,B \\ 2\,B \\ \vdots \\ (\alpha-2)\,B \end{array}\right\}$	$\cdots$	$(\alpha-1)\,A$ $\left\{\begin{array}{c} 0\,B \\ 1\,B \end{array}\right\}$	αA

5. The rate for this process can be given by

$$T_5 = y_B p_v \left[1 - \left(p_v + p_B\right)^{\alpha}\right] \ . \tag{7}$$

With these rates we can write the gain and loss equations for the densities. For the density of the empty sites we have

$$\begin{aligned} \frac{dp_v}{dt} &= -T_1 + T_2 + T_3 - T_4 + T_5 \\ &= y_B p_v - 2y_B p_v \left(p_v + p_B\right)^{\alpha} + y_A p_v \left(S_\alpha - p_v^{\alpha}\right) \ , \end{aligned} \tag{8}$$

where

$$S_\alpha = \sum_{j=1}^{\alpha} \sum_{i=0}^{\alpha-j} C_{\alpha,j}\, C_{\alpha-j,i}\, p_v^{\alpha-i-j} \left(p_A^i\, p_B^j + p_A^j\, p_B^i\right) \left(\frac{j}{i+j}\right) \ . \tag{9}$$

After some algebraic manipulations we get $S_\alpha = 1 - p_v^{\alpha}$. The Eq. (8) can be written as

$$\frac{dp_v}{dt} = p_v \left[1 - 2y_B \left(p_B + p_v\right)^{\alpha} - 2y_A p_v^{\alpha}\right] \ . \tag{10}$$

This equation presents two stationary solutions, $p_v = 0$ and

$$1 - 2y_B \left(p_v + p_B\right)^{\alpha} - 2y_A p_v^{\alpha} = 0 \ . \tag{11}$$

The solution $p_v = 0$ indicates that the system evolves to a B-poisoned state, because the $B - B$ reaction is forbidden. The other solution, Eq. (11), accounts for the reactive steady state, for which $p_v \neq 0$. Therefore, there must be a critical value of the parameter y_A, for which the system changes from a reactive steady state to an absorbing one. Let us suppose that the system is poisoned, and it is in the vicinity of the critical value y_{A_c}. By slightly changing the parameter y_A across the transition point, we allow for the appearance of some vacant sites. In this case, we can approximate Eq. (2) by $p_v + p_B \approx 1$ and the Eq. (11) furnishes

$$p_v = \left(1 - \frac{1}{2y_A}\right)^{\frac{1}{\alpha}} \ , \tag{12}$$

which gives the value $1/2$ for the critical value of the parameter y_A. For values of y_A that are less than the critical, the system always evolves to a B-poisoned state whatever the initial condition we consider. The transition between the B-poisoned state and the active steady state is described by a continuous phase transition, whose order parameter is the fraction of empty sites (p_v), and the associated critical exponent β is defined by the equation

$$p_v \sim \left(y_A - y_{A_c}\right)^{\beta} \ . \tag{13}$$

This mean-field approximation, at the site level, gives $\beta = 1/\alpha$.

B. Pair approximation

In the pair mean-field approximation we introduce the correlation between two nearest neighbor sites of the lattice by defining the conditional probability $P\left(i \,|\, j\right)$, which

is the probability that a given site to be of type i, given that one of its nearest neighbors is of type j. We define the pair probability $p_{ij} = p_j P(i \mid j)$, that a randomly chosen nearest neighbor pair of sites are occupied by the i and j monomers or they are vacant. The dynamics of the model is given by the rate of change of these pair probabilities, which are evaluated by counting the changes in the number of nearest neighbor pairs in a neighborhood of sites centered on, and including, the center pair $i - j$.

We need to consider only the pair probabilities p_{vv}, p_{vA}, p_{vB} and p_{BB} to describe this model, since the pairs $i - j$ and $j - i$, although physically distinct, they contribute with the same weight to the equations of motion. The pair probabilities are related to the densities of monomers and to the fraction of vacant sites by the relation $p_j = \sum_i p_{ij}$. We may write the following relations

$$p_A = p_{vA} \ , \tag{14}$$

$$p_B = p_{vB} + p_{BB} \ , \tag{15}$$

$$p_v = p_{vA} + p_{vB} + p_{vv} \ . \tag{16}$$

Because of the relation given by Eq. (2) we can also write

$$p_{vv} + p_{BB} + 2\left(p_{vA} + p_{vB}\right) = 1 \ . \tag{17}$$

In this pair mean-field approximation we also suppose that these pair probabilities are all statistically independent and that the system is translationally invariant. The table III show all the possible transitions among the pairs.

Table III. Possible transitions among different configurations of pairs of nearest neighbors in the lattice.

From → / To ↓	$v-v$	$v-A$	$v-B$	$B-B$
$v-v$	×	T_3	T_4	×
$v-A$	T_1	×	×	×
$v-B$	T_2	×	×	T_6
$B-B$	×	×	T_5	×

For instance, the transition T_1 means that the central pair is in the configuration $v - v$ (both sites are empty) and there is an A monomer arriving at the right site of the central pair $v - v$, changing its configuration to $v - A$. The transition probability for this event is the same as that for the transition $v - v \ \rightarrow \ A - v$, since the pairs $A - v$ and $v - A$ occur with the same probability. To calculate the transition probabilities we proceed in a manner similar to that used in the site mean-field approximation, but now they are more involved. Examples of the application of this pair approximation can be found in the references [34] and [35]. In particular, in the appendix B of the reference [34], a detailed description of the method used here is given, with emphasis to the $NO + CO$ reaction model. The reaction probability Π_{AA} was defined as being the probability of an arriving A monomer to react with anyone of its nearest neighbor A on the lattice, in the presence of the B monomers. Now, it must be replaced by the probability of reacting with another selected A monomer, in the presence of the B monomers. Then, $\pi_{AA} = \Pi_{AA}/N_A = \Pi_{AB}/N_B = 1/(N_A + N_B)$. In this case, $\pi_{AA} = \pi_{AB}$, and the reaction probabilities are the same. Thus, the transition probability for the process T_1 is very simple and it is given by

$$T_1 = y_A p_{vv} \left(\frac{p_{vv}}{p_v}\right)^{\alpha - 1} \ , \tag{18}$$

while, for the process T_3, the calculation is more involved. In this case, we have to consider two possible paths: monomer $A(B)$ arriving at the vacant site of the central pair or arriving in a nearest neighbor site of the A monomer of the central pair. In each case, all the possible distributions of A and B monomers in the neighborhood of the central pair must be taken into account. For this rate it is not trivial to write a single expression valid for any value of the coordination number α. The rate T_3 is given by

$$T_3 = p_{vA}\left(1 + \frac{p_{vv}}{p_v} + y_B \frac{p_{vB}}{p_v}\right) \ , \tag{19}$$

for the linear chain, and

$$\begin{aligned} T_3 = {} & 4 y_A p_{vA} \left[\left(\frac{p_{vv}}{p_v}\right)^3 + \frac{3}{2}\frac{p_{vB}}{p_v}\left(\frac{p_{vv}}{p_v}\right)^2 + \left(\frac{p_{vB}}{p_v}\right)^2 \frac{p_{vv}}{p_v} + \frac{1}{4}\left(\frac{p_{vB}}{p_v}\right)^3\right] + \\ & 12 y_A p_{vA} \left\{\frac{p_{vA}}{p_v}\left[\frac{1}{2}\left(\frac{p_{vv}}{p_v}\right)^2 + \frac{2}{3}\frac{p_{vB}}{p_v}\frac{p_{vv}}{p_v} + \frac{1}{4}\left(\frac{p_{vB}}{p_v}\right)^2\right] + \left(\frac{p_{vA}}{p_v}\right)^2 \left(\frac{1}{3}\frac{p_{vv}}{p_v} + \frac{1}{4}\frac{p_{vB}}{p_v}\right)\right\} + \\ & 4 y_B p_{vA} \left[\left(\frac{p_{vv}}{p_v} + \frac{p_{vB}}{p_v}\right)^3 + \frac{3}{2}\frac{p_{vA}}{p_v}\left(\frac{p_{vv}}{p_v} + \frac{p_{vB}}{p_v}\right)^2 + \left(\frac{p_{vA}}{p_v}\right)^2 \left(\frac{p_{vv}}{p_v} + \frac{p_{vB}}{p_v}\right) + \frac{1}{4}\left(\frac{p_{vA}}{p_v}\right)^3\right] \ , \end{aligned} \tag{20}$$

for the square lattice. For the case of the cubic lattice it becomes

$$T_3 = 6\left(T_{31} + T_{32}\right) \ , \tag{21}$$

where

$$\begin{aligned} T_{31} = {} & y_A p_{vA}\left[\left(\frac{p_{vv}}{p_v}\right)^5 + \frac{5}{2}\frac{p_{vB}}{p_v}\left(\frac{p_{vv}}{p_v}\right)^4 + \frac{10}{3}\left(\frac{p_{vB}}{p_v}\right)^2\left(\frac{p_{vv}}{p_v}\right)^3 + \frac{10}{4}\left(\frac{p_{vB}}{p_v}\right)^3\left(\frac{p_{vv}}{p_v}\right)^2\right] + \\ & y_A p_{vA}\left\{\left[\left(\frac{p_{vB}}{p_v}\right)^4\frac{p_{vv}}{p_v} + \frac{1}{6}\left(\frac{p_{vB}}{p_v}\right)^5\right] + 5\frac{p_{vA}}{p_v}\left[\frac{1}{2}\left(\frac{p_{vv}}{p_v}\right)^4 + \frac{4}{3}\frac{p_{vB}}{p_v}\left(\frac{p_{vv}}{p_v}\right)^3 + \frac{6}{4}\left(\frac{p_{vB}}{p_v}\right)^2\left(\frac{p_{vv}}{p_v}\right)^2\right]\right\} + \\ & 10 y_A p_{vA}\left(\frac{p_{vA}}{p_v}\right)^2\left[\frac{1}{3}\left(\frac{p_{vv}}{p_v}\right)^3 + \frac{3}{4}\frac{p_{vB}}{p_v}\left(\frac{p_{vv}}{p_v}\right)^2 + \frac{3}{5}\frac{p_{vv}}{p_v}\left(\frac{p_{vB}}{p_v}\right)^2 + \frac{1}{6}\left(\frac{p_{vB}}{p_v}\right)^3\right] + \\ & 5 y_A p_{vA}\frac{p_{vA}}{p_v}\left[\frac{4}{5}\frac{p_{vv}}{p_v}\left(\frac{p_{vB}}{p_v}\right)^3 + \frac{1}{6}\left(\frac{p_{vB}}{p_v}\right)^4\right] \ , \end{aligned} \tag{22}$$

and

$$\begin{aligned} T_{32} = {} & y_B p_{vA}\left[\left(\frac{p_{vv}+p_{vB}}{p_v}\right)^5 + \frac{5}{2}\frac{p_{vA}}{p_v}\left(\frac{p_{vv}+p_{vB}}{p_v}\right)^4 + \frac{10}{3}\left(\frac{p_{vA}}{p_v}\right)^2\left(\frac{p_{vv}+p_{vB}}{p_v}\right)^3\right] + \\ & y_B p_{vA}\left[\frac{10}{4}\left(\frac{p_{vA}}{p_v}\right)^3\left(\frac{p_{vv}+p_{vB}}{p_v}\right)^2 + \left(\frac{p_{vA}}{p_v}\right)^4\frac{p_{vv}+p_{vB}}{p_v} + \frac{1}{6}\left(\frac{p_{vA}}{p_v}\right)^5\right] \ . \end{aligned} \tag{23}$$

For instance, the gain-loss equation for the p_{vB} and p_{vv} pair densities are given by

$$\frac{dp_{vB}}{dt} = T_2 + T_6 - T_4 - T_5 \ , \tag{24}$$

$$\frac{dp_{vv}}{dt} = 2\left(T_3 + T_4 - T_1 - T_2\right) \ . \tag{25}$$

The set of equations for the pair probabilities cannot be solved analytically in any dimension. However, if we take, as in the site approximation, $p_v + p_B \cong 1$, the set of equations can be simplified near the critical point. Through the Maple manipulations for the stationary state ($\frac{dp_v}{dt} = 0$ and $\frac{dp_B}{dt} = 0$) we found that $p_v \sim \left(y_A - y_{A_c}\right)^\beta$ with $\beta = 1$ in all dimensions. This was indeed expected since the model has a similar behavior as the $A + A \rightarrow A_2$ autocatalytic model. In that model, Aukrust, Browne and Webman [28] also found the same value $\beta = 1$ for the critical exponent of the order parameter in the pair mean field approximation. We have also found the critical value of the parameter y_A. Its critical value is $y_{A_c}(d=1) = 0.5593$, $y_{A_c}(d=2) = 0.5182$ and $y_{A_c}(d=3) = 0.5050$.

In Figs. 1(a), 1(b) and 1(c) we show the mean-field results along with the Monte Carlo simulations, for the order parameter p_v for the linear, square and cubic lattices. This figure clearly indicates that a close agreement between the results of mean-field and Monte Carlo calculations is observed far away of the critical point. As we can see in Figs. 1(b) and 1(c) the critical point obtained in the pair approximation and through Monte Carlo simulations are almost the same. However, the slope of the curves at the critical point are rather different. The simulations will be detailed in the next section. For $y_A > y_{A_c}$ the system is in an active steady state, while for values $y_A < y_{A_c}$ the system is trapped into an absorbing state, where the surface is completely poisoned by monomers of the species B.

III Static Monte Carlo simulations

In this section we give a brief description of the method we used. The results of simulations were obtained through the following algorithm: we randomly choose a site from the list of empty sites of the lattice and select, with probability y_A, a monomer A to be adsorbed. If no one of the nearest neighbor sites of the selected site are occupied by A nor B monomers, then this empty site becomes occupied by a monomer A and the number of empty sites is decreased by one. Else, if there are some monomers in its neighborhood, then a reaction ($A+A$) or ($A+B$) will take place with probability Π_{AA} (Π_{AB}), and the list of empty sites is increased by one. On the other hand, with probability $y_B = 1 - y_A$, a B monomer is deposited on the empty site. Then, we search for A monomers in its neighborhood. If more than one A monomer is found, we randomly choose which one will react with B, leaving two empty sites after reaction. If no

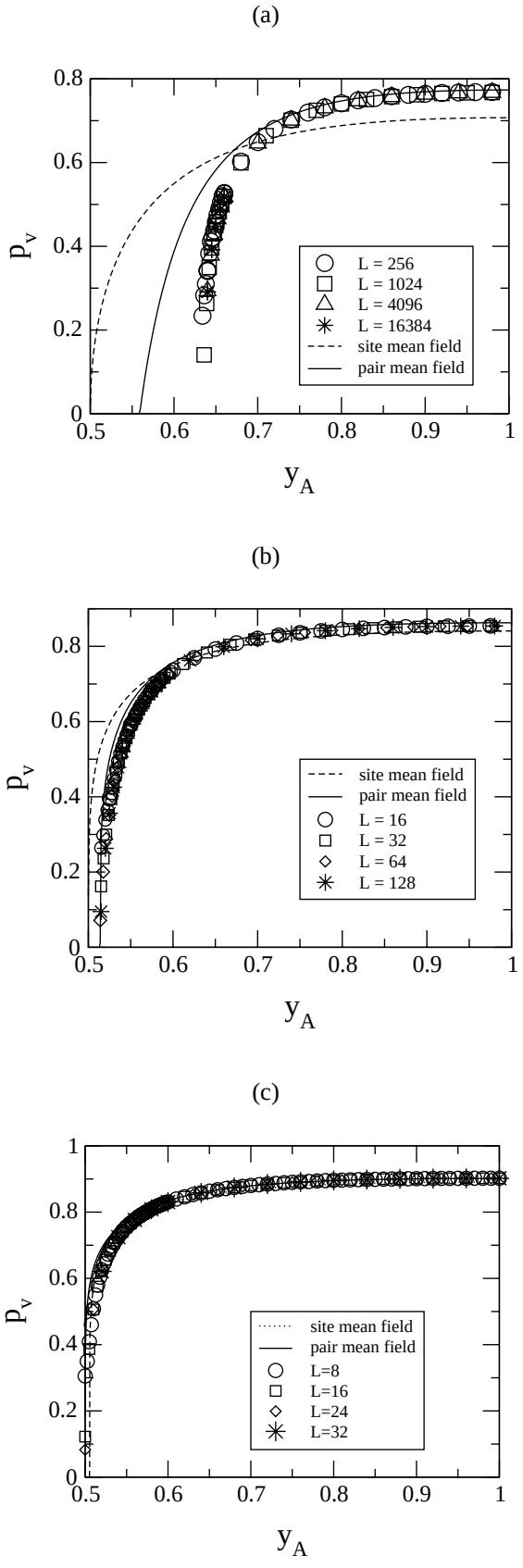

Figure 1. Fraction of empty sites as a function of the parameter y_A. The solid and dotted lines correspond to the mean field approximations. The symbols represent the results of Monte Carlo simulations for various lattice sizes L. Linear lattice (a), square lattice (b) and cubic lattice (c).

A monomer is found, then B remains adsorbed. In order to improve the efficiency of the algorithm we use a continuous time Monte Carlo procedure, where the time per event is no longer constant. If at a given instant of time the number of vacant sites is N_v, the selection from this list corresponds to a time increment N_v^{-1}. All the simulations started with an empty lattice and the time required for a finite system to become poisoned depends on the lattice size and on the value of y_A. For the lattice sizes we consider, we expect that, due to the fluctuations, a surface fully covered will be observed for any value of y_A for sufficiently long times. The absorbing state is the only stable state. However, for y_A larger than the critical value, the system can be found in a reactive steady state, until a large fluctuation drive it to a poisoned state. This reactive steady state is indeed a metastable state. For these metastable states we compute the order parameter (fraction of vacant sites) which exhibits fluctuations around the mean value. We performed simulations for the various lattice sizes, and we considered detailed calculations near the transition point. The simulations showed that the system exhibits a continuous phase transition between an absorbing state, which is poisoned by monomers of the type B, and an active steady state.

To obtain the critical exponents of the model we performed a finite-size scaling analysis for the order parameter p_v. We assume that it is a generalized homogeneous function of the variables L and $\Delta = y_A - y_{Ac}$. We suppose [18, 28] that in the critical region, the order parameter behaves as

$$p_v \sim L^{-\beta/\nu_\perp} \Phi \left(\Delta L^{1/\nu_\perp} \right) \ , \qquad (26)$$

where Φ is a scaling function with the properties that at the critical point $\Phi(0) \sim 1$, and that $\Phi(x) \sim x^\beta$, for $x \to \infty$. The latter property recovers the power law behavior of Eq. (13) which is valid for a system of infinite size near its critical point. The exponent $\nu_\perp$ is the correlation length exponent and measures the correlations of the order parameter over the surface. At the critical point, a log-log plot of p_v versus L must be a straight line with slope $-\beta/\nu_\perp$. Figs. 2(a), 2(b) and 2(c) show the log-log plots of p_v versus L, for the linear, square and cubic lattices, respectively. The error bar for each point is not included in these plots. The data points give the value $y_{A_c}(d=1) = 0.63743(7)$, $y_{A_c}(d=2) = 0.5140(5)$ and $y_{A_c}(d=3) = 0.5004(1)$ for the critical value of the parameter y_A for the three lattices. The values of the critical exponent ratio are $\beta/\nu_\perp = 0.25(1)$, $0.80(2)$ and $1.40(2)$, for the linear, square and cubic lattices, respectively. These values were calculated by linear fittings to the data points of the simulations including their error bars.

In order to carry out a finite-size scaling analysis for the order parameter, a number of independent runs were done near the transition point for each lattice size, and for $d = 1$, 2 and 3. Data obtained from the quasiequilibrium active steady states were then sampled. For instance, for the lattice size $L = 128$ and for the square lattice, we determined the averages and the corresponding fluctuations from a set

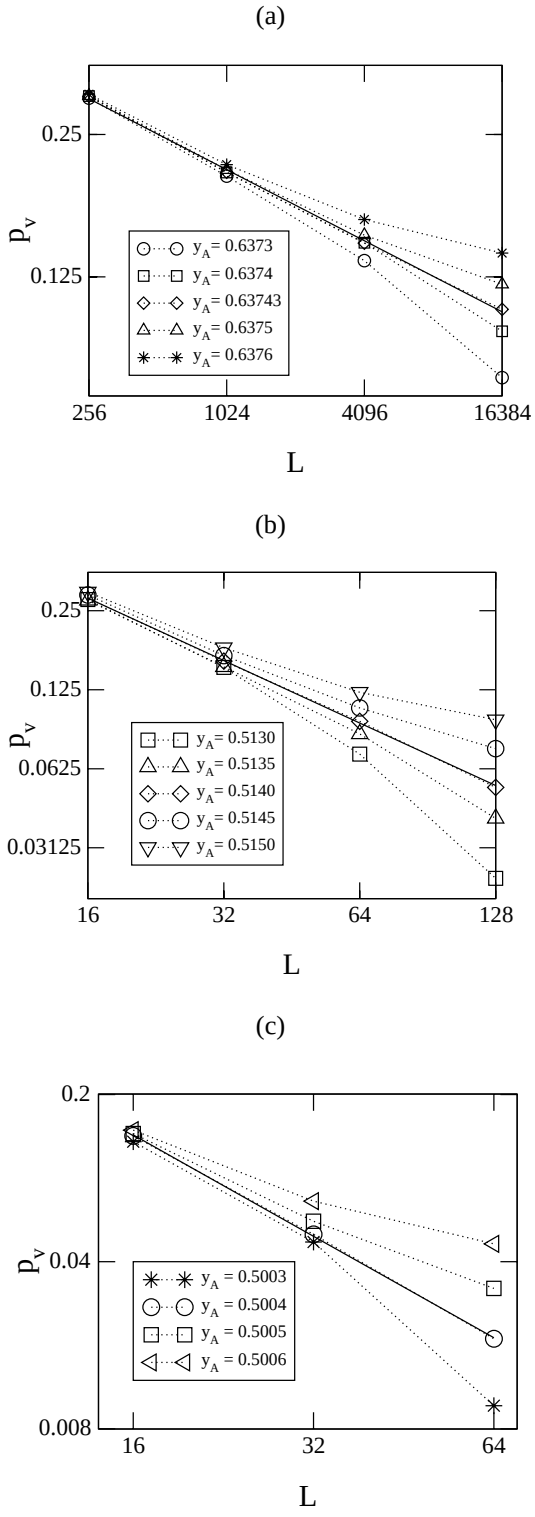

Figure 2. Log-log plots of p_v versus L for some values of the parameter y_A (indicated in the figures), near the critical point, for (a) linear chain, (b) square lattice, and (c) cubic lattice. From the slope of the straight lines we found $\beta/\nu_\perp = 0.25$, 0.80 and 1.40, for the linear, square and cubic lattices, respectively.

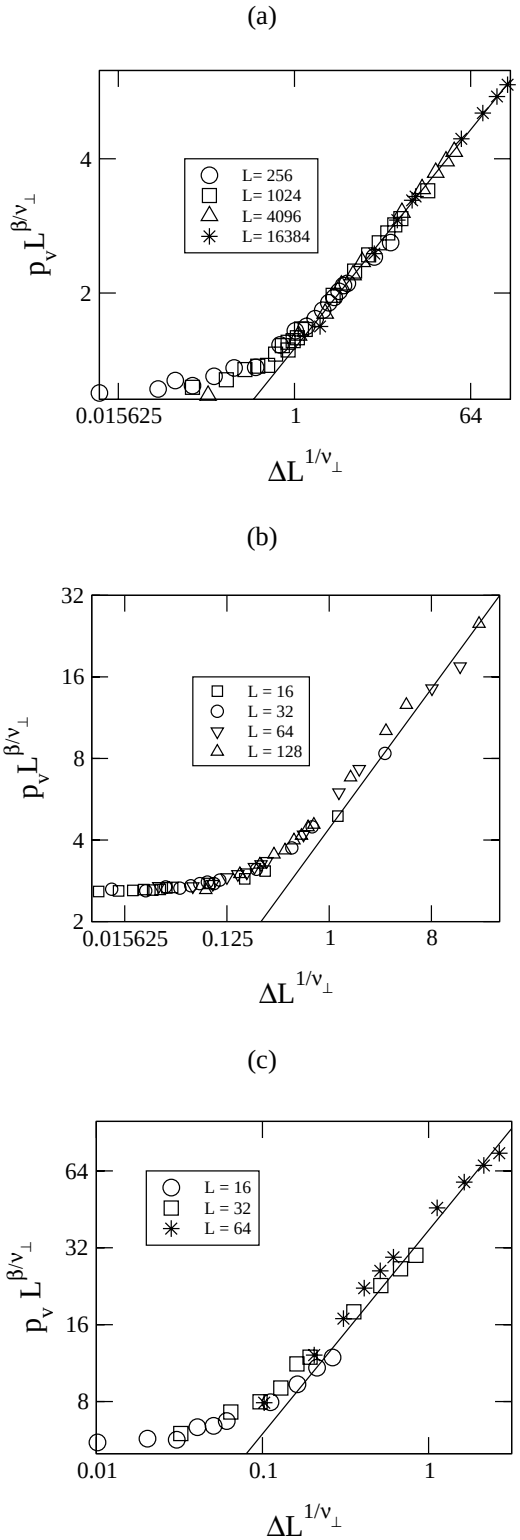

Figure 3. Collapse of the data points for the order parameter p_v for different lattice sizes L for the linear chain (a), square (b) and cubic (c) lattices. The figure is a log-log plot of $p_v L^{\beta/\nu_\perp}$ versus $\Delta L^{1/\nu_\perp}$. The slope of the solid lines, which is the asymptotic behavior of $p_v L^{\beta/\nu_\perp}$, gives $\beta = 0.27$, 0.57 and 0.80 for the linear, square and cubic lattices, respectively.

of 100 surviving samples. We have plotted, in Fig. 3, the quantity $p_v L^{\beta/\nu_\perp}$ versus $\Delta L^{1/\nu_\perp}$ in a log-log scale, for various lattice sizes and dimensions. Figs. 3(a), 3(b) and 3(c) correspond to the simulations performed for the linear, square and cubic lattices, respectively. As we can see, the data for the different lattice sizes, in each plot, collapse very well, suggesting the correctness of the scaling form of Eq. (26). Thus, for large values of the argument of the function Φ in Eq. (26), the data should fall on a straight line with slope β.

The collapse of the data points was obtained with the following values of the parameters: $\beta = 0.27(2)$, $\nu_\perp = 1.07(3)$ and $y_{A_c} = 0.6375(1)$ for the linear chain, $\beta = 0.58(3)$, $\nu_\perp = 0.72(5)$ and $y_{A_c} = 0.5141(2)$ for the square lattice, and $\beta = 0.80(1)$, $\nu_\perp = 0.58(1)$ and $y_{A_c} = 0.5004(1)$ for the cubic lattice. We observe that the ratios $\beta/\nu_\perp$ are the same as those found in Fig. 2. The best values of the static critical exponents of the Directed Percolation [36] are listed in the table IV.

Table IV. Best values for the static critical exponents of the directed percolation universality class.

critical exponent	$d=1$	$d=2$	$d=3$
β	0.276486(8)	0.584(4)	0.81(1)
$\nu_\perp$	1.096854(4)	0.734(4)	0.581(5)

As we can see, there is a good agreement between the values we found in our static Monte Carlo simulations and those of the DP. This is a good evidence that our catalytic reaction model with competing reactions is in the same universality class of the Directed Percolation.

IV Dynamic Monte Carlo simulations

We also studied the dynamical critical behavior of the model by introducing a suitable time variable. It is defined as being the mean time required for the system to become completely poisoned. Firstly, we define the time for a selected sample to become poisoned, that is,

$$\tau_s = \frac{\sum_t t p_v}{\sum_t p_v} \quad . \tag{27}$$

This particular function depends on the linear size L of the system and on the parameter y_A. Then, we take an average over all the independent samples, getting the quantity $\tau =< \tau_s >_s$, which is assumed to have the scaling form [18, 28]

$$\tau \sim L^z \phi\left(\Delta L^{1/\nu_\perp}\right) \quad . \tag{28}$$

Albano and Marro [37] have proposed a phenomenological scaling approach for the poisoning time at the first order transition of the monomer-dimer reaction model. In their approach this time diverges logarithmically with the linear lattice size and algebraically with the distance to the coexistence point. In Eq. (28) the scaling function ϕ is assumed to behave as $\phi(0) \sim 1$ at the critical point, so that a log-log plot of τ versus the system size L is a straight line with the slope z. This result is displayed in our Fig. 4 for the linear chain (a), square (b) and cubic (c) lattices. From these figures we obtain $z = 1.54(5)$ and $y_{A_c} = 0.6375(1)$ for the linear chain, $z = 1.68(6)$ and $y_{A_c} = 0.5142(2)$ for the square lattice, and $z = 1.94(2)$ and $y_{A_c} = 0.5006(1)$ for the cubic lattice. Eq. (28) must be consistent with the definition of the $\nu_{||}$ exponent: in the limit of a system with an infinite lattice size ($L \to \infty$) the characteristic time diverges as $\tau \sim (y_A - y_{A_c})^{-\nu_{||}}$. So, the z and the $\nu_{||}$ exponents are related by $z = \nu_{||}/\nu_\perp$.

Another way to get information about the critical exponents at the critical point, is to consider, for a fixed time t, all the samples (the surviving ones and those which entered the absorbing state). Defining δ as the average of the order parameter over many samples, this quantity will depend only on the system size L and on time. For the long time behavior and for a large system size one can assume the following scaling form

$$\delta \sim L^{-\beta/\nu_\perp} \psi\left(t/L^z\right) \quad . \tag{29}$$

We have plotted, in Fig. 5, $\delta L^{\beta/\nu_\perp}$ versus t/L^z on a log-log scale. The data points collapse very well for $\beta/\nu_\perp = 0.25(1)$, $z = 1.55(2)$ and $y_{A_c} = 0.6375(1)$ in the linear chain case. The values used for the square lattice were $\beta/\nu_\perp = 0.80(1)$, $z = 1.66(7)$ and $y_{A_c} = 0.5141(1)$. In the cubic lattice the collapse was obtained by choosing $\beta/\nu_\perp = 1.40(1)$, $z = 1.95(1)$ and $y_{A_c} = 0.5005(2)$. All these values are consistent with the previous ones we have found by employing the other manner of collapsing the order parameter data. As we can see from these figures, for $t < L^z$ the data points collapse onto a straight line with the slope $-\beta/\nu_{||} = -0.15(1)$, $-0.48(2)$ and $-0.71(4)$ for the linear chain, square and cubic lattices, respectively. Finally, from these ratios, we can estimate the value of the critical exponent $\nu_{||}$. We found the values $1.8(1)$ for the linear chain, $1.21(8)$ for the square lattice and $1.13(8)$ for the cubic lattice. In Fig. 5(c), the data fall on a straight line only in a small region. This fact is due to small lattice sizes used in $d = 3$.

Another way of studying the dynamical critical behavior of the model is by employing an epidemic analysis [29, 30, 31]. We measured the survival probability $P(t)$, the number of empty sites $n_v(t)$, and the mean square displacement from the origin $R^2(t)$, from an initial state containing only a single empty site at the center of the lattice. Then, we followed the time evolution of many samples with this initial condition until a maximum time $t_{max} = 10000$ time steps in the linear chain case, $t_{max} = 2500$ time steps for the square lattice, and $t_{max} = 5000$ time steps for the cubic lattice. For the linear chain and square lattice, one time step was defined by 100 changes in the configuration of the system, which could be an adsorption or a chemical reaction event. For the cubic lattice, one time step was defined by 10 changes in the configuration of the system. We have taken a lattice of size $L = 5 \times 10^5$ for the linear chain, while for the square and cubic lattices, we took $L = 1000$ and $L = 50$, respectively. $P(t)$ and $R^2(t)$ are averaged only for those configurations that have not entered into the absorbing state until the time t, and $n_v(t)$ is averaged over all the samples [13]. To get a good statistics we need to run at least 2.5×10^6 independent samples in all dimensions.

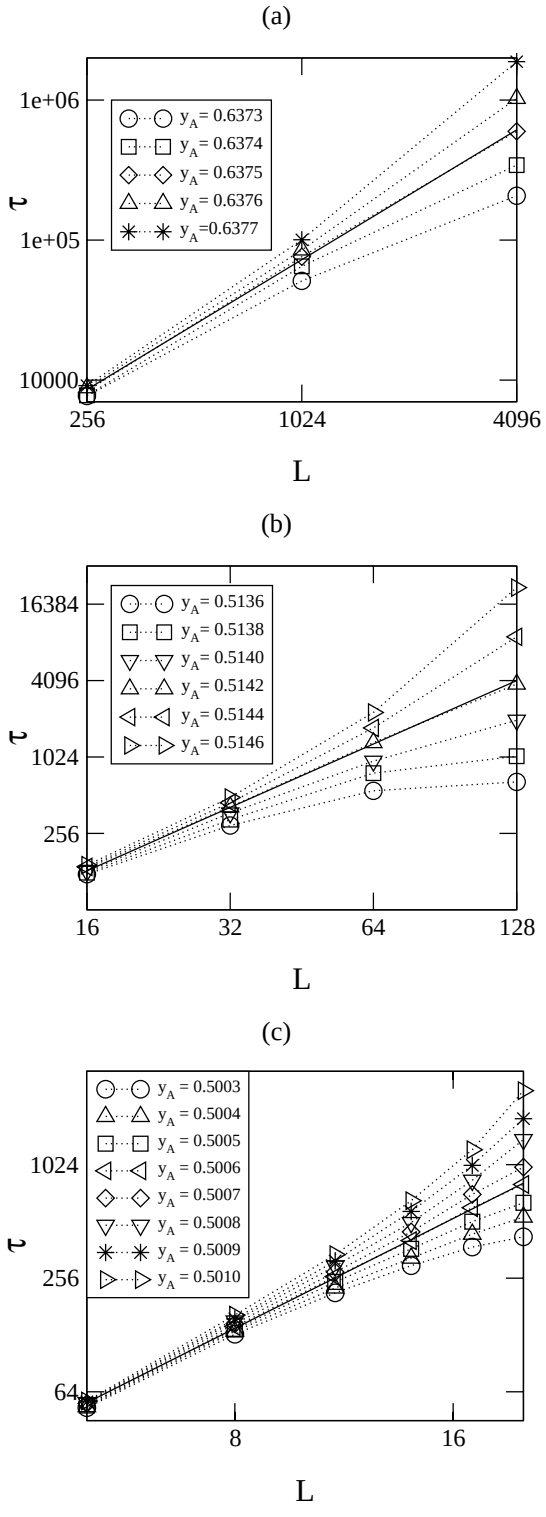

Figure 4. Log-log plots of τ versus L for some values of the parameter y_A (indicated in the figures), near the critical point. In figure (a), for the linear chain, the slope of the straight line gives $z = 1.54$, while for the square (b) and cubic (c) lattices, z is 1.68 and 1.94, respectively.

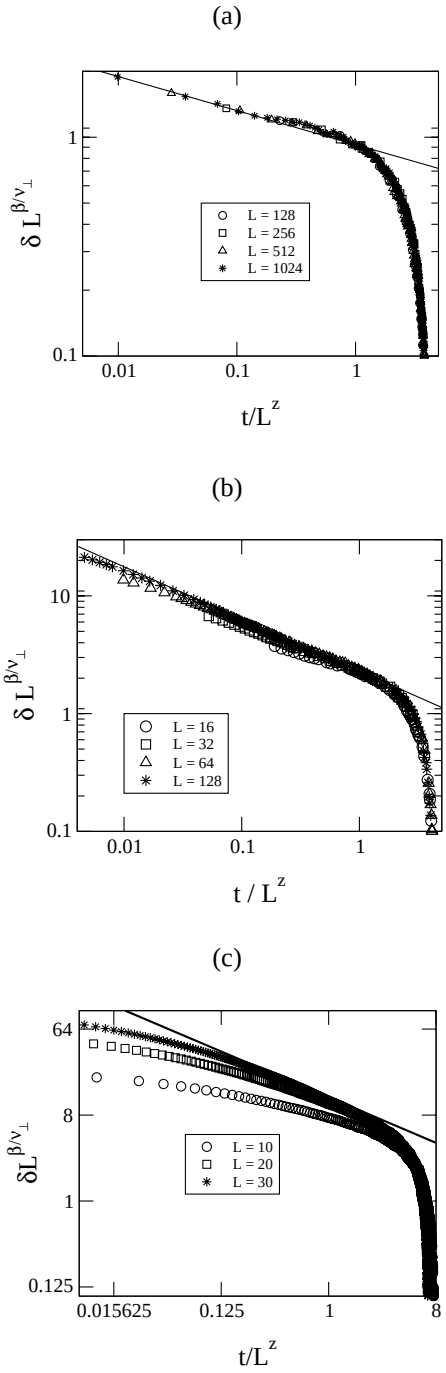

Figure 5. Collapse of the data points for the dynamical behavior of the order parameter at the critical point. For the linear chain (a), a good collapse was obtained with $\beta/\nu_\perp = 0.25$, $z = 1.55$, and $y_{A_c} = 0.6375$. The slope of the straight line is $\beta/\nu_{||} = 0.15$. A good collapse is obtained for the square lattice (b), with the values $\beta/\nu_\perp = 0.80$, $z = 1.66$ and $y_{A_c} = 0.5141$. The slope of the straight line gives $\beta/\nu_{||} = 0.48$. In the case of cubic (c) lattice we found $\beta/\nu_\perp = 1.40$, $z = 1.95$ and $y_{A_c} = 0.5005$. The slope of the straight line gives $\beta/\nu_{||} = 0.71$.

From the scaling ansatz for the DP class and similar models [38, 39], the physical quantities of interest depend on the relevant parameters $\vec{r}$, t and $\Delta = y_A - y_{A_c}$, only through the scaling variables $r^2 t^{-\zeta}$ and $\Delta t^{1/\nu_{||}}$, times some power of r^2, t or Δ. In the scaling regime, the local fraction of empty sites, averaged over all trials, surviving or not, can be written as

$$p_v\left(\vec{r},t\right) \sim t^{\eta-\zeta d/2} F\left(r^2 t^{-\zeta}, \Delta t^{1/\nu_{||}}\right) \quad , \tag{30}$$

and the survival probability is expected to behave as

$$P\left(t\right) \sim t^{-\delta} \Phi\left(\Delta t^{1/\nu_{||}}\right) \quad , \tag{31}$$

where $\nu_{||}$ is the critical exponent associated with the divergence of the temporal correlation length. From equation Eq. (30) we can calculate the number of empty sites, $n_v\left(t\right)$, and the mean square spreading of the origin, $R^2\left(t\right)$,

$$n_v\left(t\right) = \int p_v\left(\vec{r},t\right) d^d r \quad , \tag{32}$$

$$R^2\left(t\right) = \frac{1}{n_v\left(t\right)} \int r^2 p_v\left(\vec{r},t\right) d^d r \quad . \tag{33}$$

These equations can be cast in the following form

$$n_v\left(t\right) \sim t^{\eta} \Psi\left(\Delta t^{1/\nu_{||}}\right) \quad , \tag{34}$$

$$R^2\left(t\right) \sim t^{\zeta} \Theta\left(\Delta t^{1/\nu_{||}}\right) \quad . \tag{35}$$

Here, δ, η and ζ are the dynamical critical exponents of the model. The exponent ζ is related to the critical exponent z, that governs the divergence of the characteristic time, by $\zeta = 2/z$. Here, Φ, Ψ and Θ are scaling functions with the property that, at the critical point, they assume a constant value, that is, they are nonsingular functions at the critical point. At the critical point, Eqs. (31), (34) and (35) assume asymptotic power laws

$$P\left(t\right) \sim t^{-\delta} \quad , \tag{36}$$

$$n_v\left(t\right) \sim t^{\eta} \quad , \tag{37}$$

$$R^2\left(t\right) \sim t^{\zeta} \quad . \tag{38}$$

Log-log plots of these quantities, at the critical point, must be straight lines with slopes giving the corresponding critical exponents. These plots are shown in Figs. 6(a), 6(b) and 6(c), for the linear chain, square and cubic lattices, respectively. In each plot of Fig. 6(a) we have three curves. Each curve, from top to bottom, is associated with the values $y_A = 0.6376$, $y_A = 0.6375$ and $y_A = 0.6374$. The straight line gives the critical value $y_{A_c}(d=1) = 0.6375(1)$. From each plot we obtain $\delta = 0.160(3)$, $\eta = 0.314(2)$ and $\zeta = 1.260(1)$. In each plot of Fig. 6(b) the curves were built with the values $y_A = 0.5145$, 0.5142 and 0.5139. The critical value is $y_{A_c} = 0.5142(3)$ and the dynamical critical exponents in two dimensions are $\delta = 0.47(1)$, $\eta = 0.23(1)$ and $\zeta = 1.12(1)$. For the Fig. 6(c) the curves, from top to bottom correspond to the values $y_A = 0.5005$, $y_A = 0.5004$ and $y_A = 0.5003$ and the dynamical critical exponents are $\delta = 0.71(4)$, $\eta = 0.09(7)$ and $\zeta = 1.03(1)$.

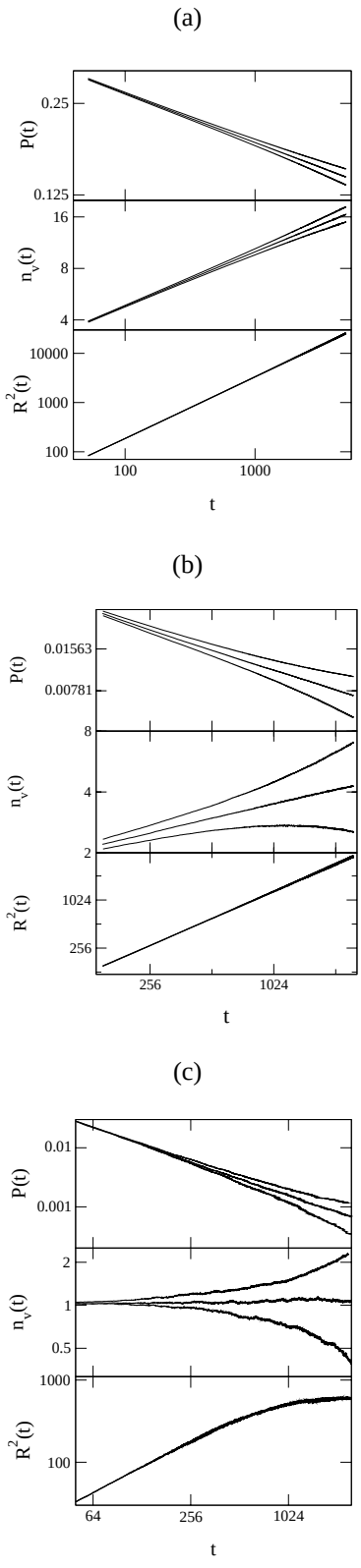

Figure 6. Log-log plots for the quantities $P\left(t\right)$, $n_v\left(t\right)$ and $R^2\left(t\right)$ for the linear (a), square (b) and cubic (c) lattices. From these figures we get the corresponding critical values $y_{A_c}(d=1) = 0.6375$, $y_{A_c}(d=2) = 0.5142$ and $y_{A_c}(d=3) = 0.5004$.

It is also possible to find the values of the critical exponents by looking at the local slopes. Consider, for instance, Eq. (31). By changing the scale of the time variable by an integer m we can write, at the critical point, $P(mt) = m^{-\delta} P(t)$. From this, we have

$$-\delta(t) = \frac{\log\left[P(mt)/P(t)\right]}{\log m} \quad , \tag{39}$$

with similar expressions for the exponents η and ζ. At large times, the local slope $\delta(t)$ assumes the following asymptotic behavior

$$\delta(t) = \delta + at^{-\theta} + bt^{-\phi} + \cdots \quad , \tag{40}$$

where θ and ϕ are corrections to scaling due to the finite size of the lattice. We also estimated the critical exponents by plotting the local slopes versus $1/t$ and extrapolating to $1/t \to 0$. The plots for the local slope $\delta(t)$ are shown in Fig. 7(a), for the linear chain, in Fig. 7(b), for the square lattice and in Fig. 7(c) for the cubic lattice, where we used $m = 2$. The curves in each plot correspond to different values of the parameter y_A around the critical value y_{A_c}, which is the central curve in the plot. From these figures we estimate the values $\delta = 0.163(7)$, $0.46(1)$ and $0.71(3)$ for the linear chain, square and cubic lattices. We also plotted the local slope $\eta(t)$ versus $1/t$ for the three lattices in the Figs. 8(a), 8(b) and 8(c). From these figures $\eta(d=1) = 0.31(5)$, $\eta(d=2) = 0.23(1)$ and $\eta(d=3) = 0.12(4)$. Finally, in Fig. 9, we plotted the local slope $\zeta(t)$ versus $1/t$ for the linear chain 9(a), square 9(b) and cubic 9(c) lattices. These plots give the values $\zeta(d=1) = 1.26(1)$, $\zeta(d=2) = 1.13(2)$ and $\zeta(d=3) = 1.03(1)$.

Our calculated dynamical critical exponents agree with those found for the Directed Percolation in one, two and three spatial dimensions. The best values of these critical exponents [36] are listed in the table V.

Table V. Best values for the dynamic critical exponents of the directed percolation universality class.

critical exponent	$d=1$	$d=2$	$d=3$
z	1.580745(10)	1.76(3)	1.90(1)
$\nu_{\|\|}$	1.733847(6)	1.295(6)	1.105(5)
δ	0.159464(6)	0.451	0.73
η	0.313686(8)	0.230	0.12
ζ	1.26523	1.13636	1.05263

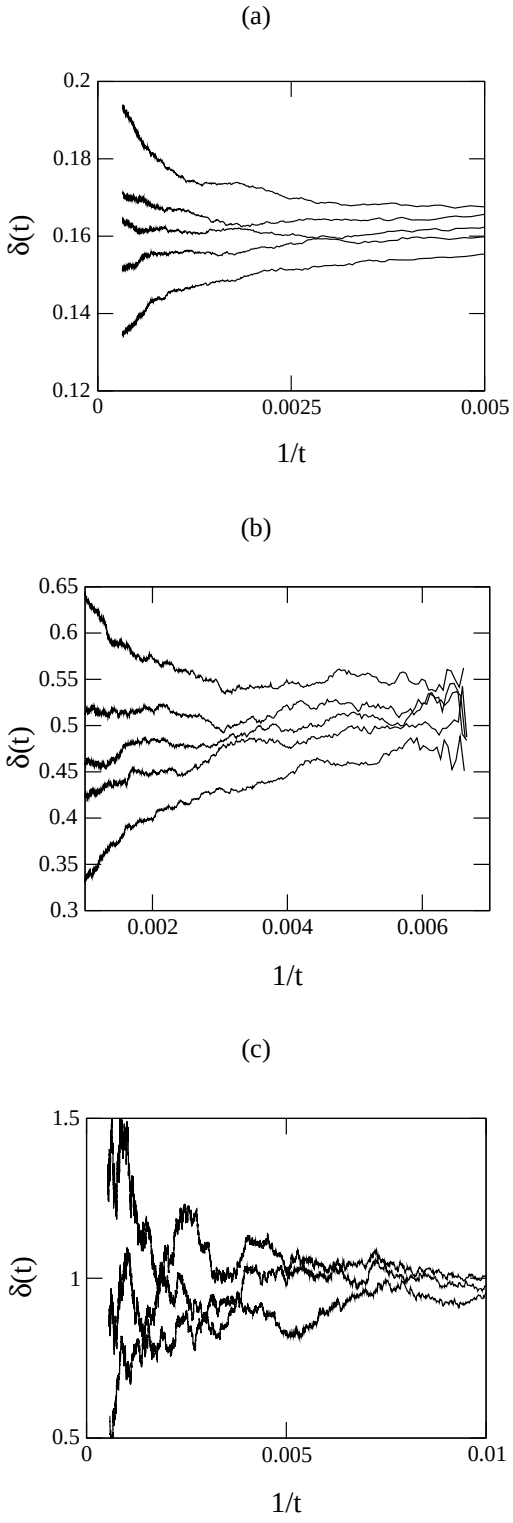

Figure 7. Local slope $\delta(t)$ for the linear chain (a), square (b) and cubic (c) lattices. From these plots we estimate the value of the critical exponent δ, whose values are $\delta(d=1) = 0.163(7)$, $\delta(d=2) = 0.46(1)$ and $\delta(d=3) = 0.71(3)$.

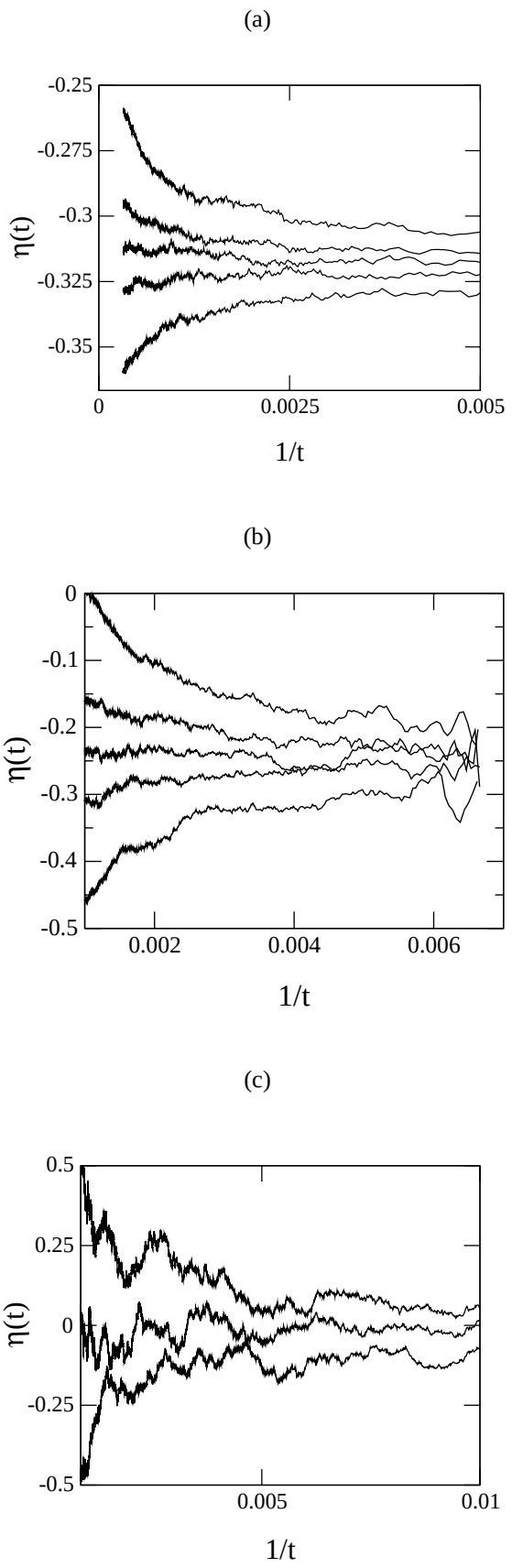

Figure 8. Local slope $\eta\,(t)$ for the linear chain (a), square (b) and cubic (c) lattices. From these plots we estimate the value of the critical exponent η, whose values are $\eta(d\,=\,1)\,=\,0.31(5)$, $\eta(d\,=\,2)\,=\,0.23(1)$ and $\eta(d\,=\,3)\,=\,0.23(12)$.

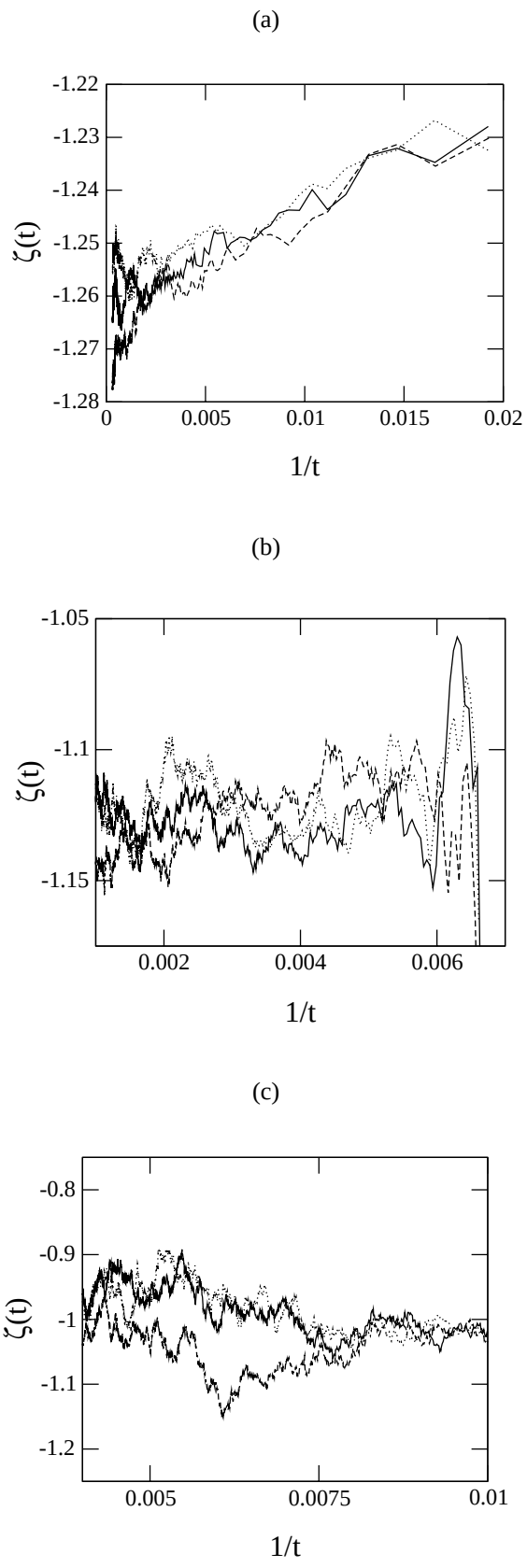

Figure 9. Local slope $\zeta\,(t)$ for the linear chain (a), square (b) and cubic (c) lattices. From these plots we estimate the value of the critical exponent ζ, whose values are $\zeta(d\,=\,1)\,=\,1.26(1)$, $\zeta(d\,=\,2)\,=\,1.13(2)$ and $\zeta(d\,=\,3)\,=\,1.03(1)$.

V Conclusions

We have studied a competitive reaction model between monomers on a catalytic surface. The model can be viewed as being a mixture of the autocatalytic and the monomer-monomer reaction models. We have considered the site and the pair mean-field approximations to obtain the steady states and a qualitative picture of the critical behavior of the model in one, two and three spatial dimensions. The model displays a continuous phase transition into a single absorbing state. The critical point obtained via pair approximation agree very well with that found by Monte Carlo simulations in two and three dimensions. By employing finite-size scaling arguments, we determined the static and dynamic critical exponents of the model. All the values we have found are in agreement with those of the Directed Percolation (DP) in $(d+1)$ dimensions. This was indeed expected, since the phase transition from the active to the single absorbing state is one in which the concentration of vacancies goes continuously to zero. Although our model can not be mapped onto the DP, they are equivalent concerning the static and dynamic critical behavior. This is a strong evidence in favor of the universality: models with different dynamical rules exhibit the same critical behavior. The essential characteristic shared by these models is a continuous phase transition into an absorbing state. The DP conjecture asserts that models with a continuous phase transition into an absorbing state belong generically to the DP universality class. In summary, based on the values we have found for the static and dynamic critical exponents, and on the DP conjecture, we can conclude that our model belongs to the same universality class of the DP.

Acknowledgments

This work was supported by the Brazilian agency CNPq.

References

[1] R. N. Mantegna and H. E. Stanley, *An Introduction to Econophysics: Correlation and Complexity in Finance*, (Cambridge University Press, Cambridge, 2000).

[2] J. V. Andersen and D. Sornette, Eur. Phys. J. B **31**, 141 (2003).

[3] R. Dickman, Phys. Rev. Lett. **90**, 108701 (2003).

[4] R. Dickman, T. Tomé and M. J. de Oliveira, Phys. Rev. E **66**, 016111 (2002).

[5] T. Tomé and M. J. de Oliveira, Phys. Rev. Lett. **86**, 5643 (2001).

[6] J. Krug, Adv. Physics **46**, 139 (1997).

[7] A. -L. Barabasi and H. E. Stanley, *Fractal concepts in surface growth*, (Cambridge University Press, Cambridge, 1995).

[8] D. Chowdhury, L. Santen, and A. Schadschneider, Phys. Rep. **329**, 199 (2000).

[9] V. S. Leite, and W. Figueiredo, Phys Rev. E **66**, 46102 (2002).

[10] W. Figueiredo and B. C. S. Grandi, Braz. J. of Phys. **30**, 58 (2000).

[11] M. Godoy, and W. Figueiredo, Phys. Rev. E **66**, 036131 (2002).

[12] Kenneth G. Wilson, Phys. Rev. B **9**, 3174 (1971); Phys. Rev. B **9**, 3184 (1971).

[13] J. Marro and R. Dickman, *Nonequilibrium phase transitions in lattice models*, (Cambridge University Press, Cambridge, 1999).

[14] *Nonequilibrium statistical mechanics in one dimension*, edited by V. Privman, (Cambridge Universty Press, Cambridge, 1997).

[15] F. Schlögl, Z. Physik **253**, 147 (1972).

[16] R. M. Ziff, E. Gulari, and Y. Barshad, Phys. Rev. Lett. **56**, 2553 (1986).

[17] R. M. Ziff, and B. J. Brosilow, Phys. Rev. A **46**, 4630 (1992); I. Jensen, H. C. Fogedby, and R. Dickman, Phys. Rev. A **41**, 3411 (1990); R. Dickman and M. Burschka, Phys. Lett. A **127**, 132 (1988); E. V. Albano, Surf. Sci. **306**, 240 (1994); J. W. Ewans, and M. S. Miesch, Phys. Rev. Lett. **66**, 833 (1991); V. S. Leite, B. C. S. Grandi, and W. Figueiredo, J. Phys. A: Math. Gen. **34**, 1967 (2001).

[18] E. C. da Costa, and W. Figueiredo, J. Chem. Phys. **117**, 331 (2002).

[19] E. C. da Costa, and W. Figueiredo, J. Chem. Phys. **118**, (2003).

[20] R. M. Ziff and K. Fichthorn, Phys. Rev. B **34**, 2038 (1986).

[21] P. Meakin and D. J. Scalapino, J. Chem. Phys. **87**, 731 (1987).

[22] P. L. Krapivsky, J. Phys. A: Math. Gen. **25**, 5831 (1992).

[23] H. Park, J. Köhler, In-Mook Kim, D. ben-Avraham and S. Redner, J. Phys. A: Math. Gen. **26**, 2071 (1993).

[24] D. ben-Avraham, D. Considine, P. Meakin, S. Redner, and H Takayasu, J. Phys. A: Math. Gen. **23**, 4297 (1990).

[25] K. S. Brown, K. E. Bassler, and D. A. Browne, Phys. Rev. E **56**, 3953 (1997).

[26] J. Cortés, H. Puschmann, and E. Valencia, J. Chem. Phys **106**, 1467 (1997).

[27] D. A. Browne and P. Kleban, Phys. Rev. A **40**, 1615 (1989).

[28] T. Aukrust, D. A. Browne, and I. Webman, Phys. Rev. A **41**, 5294 (1990).

[29] P. Grassberger, J. Phys. A **22**, 3673 (1989).

[30] I. Jensen, J. Phys. A, **26**, 3921 (1993).

[31] I. Jensen, Phys. Rev. E **50**, 3623 (1994).

[32] H. Hinrichsen, Braz. J. of Phys. **30**, 69 (2000).

[33] E. C. da Costa and W. Figueiredo, Phys. Rev. E **61**, 1134 (2000).

[34] A. G. Dickman, B. C. S. Grandi, W. Figueiredo, and R. Dickman, Phys. Rev. E **59**, 6361 (1999).

[35] G. L. Hoenicke, and W. Figueiredo, Phys. Rev. E **62**, 6216 (2000).

[36] H. Hinrichsen, Adv. Phys. **49**, 815 (2000).

[37] E. V. Albano and J. Marro, J. Chem. Phys. **22**, 10279 (2000).

[38] P. Grassberger, Z. Physik B **47**, 465 (1982).

[39] P. Grassberger and A. De La Torre, Annals of Physics **122**, 373 (1979).